Delft University of Technology

Cooperative multi-agent control for autonomous ship towing under environmental disturbances

Du, Zhe; Negenborn, Rudy R.; Reppa, Vasso

DOI
10.1109/JAS.2021.1004078

Publication date
2021

Document Version
Final published version

Published in
IEEE/CAA Journal of Automatica Sinica

Citation (APA)
Du, Z., Negenborn, R. R., & Reppa, V. (2021). Cooperative multi-agent control for autonomous ship towing under environmental disturbances. *IEEE/CAA Journal of Automatica Sinica*, *8*(8), 1365-1379. https://doi.org/10.1109/JAS.2021.1004078

Important note
To cite this publication, please use the final published version (if applicable).
Please check the document version above.

Copyright
Other than for strictly personal use, it is not permitted to download, forward or distribute the text or part of it, without the consent of the author(s) and/or copyright holder(s), unless the work is under an open content license such as Creative Commons.

Takedown policy
Please contact us and provide details if you believe this document breaches copyrights.
We will remove access to the work immediately and investigate your claim.

This work is downloaded from Delft University of Technology.
For technical reasons the number of authors shown on this cover page is limited to a maximum of 10.

Green Open Access added to TU Delft Institutional Repository

'You share, we take care!' - Taverne project

https://www.openaccess.nl/en/you-share-we-take-care

Otherwise as indicated in the copyright section: the publisher is the copyright holder of this work and the author uses the Dutch legislation to make this work public.

Cooperative Multi-Agent Control for Autonomous Ship Towing Under Environmental Disturbances

Zhe Du, Rudy R. Negenborn, and Vasso Reppa, *Member, IEEE*

***Abstract*—Among the promising application of autonomous surface vessels (ASVs) is the utilization of multiple autonomous tugs for manipulating a floating object such as an oil platform, a broken ship, or a ship in port areas. Considering the real conditions and operations of maritime practice, this paper proposes a multi-agent control algorithm to manipulate a ship to a desired position with a desired heading and velocity under the environmental disturbances. The control architecture consists of a supervisory controller in the higher layer and tug controllers in the lower layer. The supervisory controller allocates the towing forces and angles between the tugs and the ship by minimizing the error in the position and velocity of the ship. The weight coefficients in the cost function are designed to be adaptive to guarantee that the towing system functions well under environmental disturbances, and to enhance the efficiency of the towing system. The tug controller provides the forces to tow the ship and tracks the reference trajectory that is computed online based on the towing angles calculated by the supervisory controller. Simulation results show that the proposed algorithm can make the two autonomous tugs cooperatively tow a ship to a desired position with a desired heading and velocity under the (even harsh) environmental disturbances.**

***Index Terms*—Cooperative control, environmental disturbances, multiple autonomous vessels, robust control, ship towing.**

I. Introduction

In recent years, the advancements in information and communication technologies, sensor technology, as well as automatic control and computational intelligence have increased the intelligence level of transportation systems [1], [2]. For waterborne transportation, we have seen significant development of autonomous surface vessels (ASVs), whose application areas are gradually transformed from military deployment [3] and scientific research [4] to civil uses [5]. In the meanwhile, the number of controlled ASVs is increased from one to multiple to carry out more complex missions and scenarios [6]–[8], which makes the original problem become more challenging from the viewpoint of coordination [9]. Ship manipulation in or near port areas is considered one of the most sophisticated operations in waterborne transportation [10], while the environmental disturbances make it more challenging, even for the experienced captain [11].

To make the operation of ship manipulation safer and more effective, two solutions are put forward according to the concept of "smart shipping" [12]: The first is to focus on the automation of the ship itself to increase the efficiency in the shipping process [13]; The second is to involve auxiliary operations through the cooperation of autonomous marine agents to ensure the ship safety [14]. Thus, the first approach to solve the sophisticated ship manipulation problem is called self-berthing by autonomous ship, while the second approach is called assisted-berthing by multiple autonomous tugs.

A. Related Works

The classification of autonomous ship berthing, corresponding control methods, and disturbance considerations are shown in Table I; The upper half [15]–[22] is dedicated to self-berthing and lower half [23]–[31] are the assisted-berthing. Self-berthing is a single-agent under-actuated control problem, aiming to control the ship motion in 3 degrees of freedom (DoF) with usually, less number of control inputs (rudder angle and propeller revolution). For the control method, artificial neural networks (ANN) is most used [32]. Research works combine ANN with other control algorithms to get a better performance and adapt to the environment disturbances (mainly the wind influence). Combining with model predictive control (MPC) [15], a short computing time and good tracking performance method in real sea conditions is achieved. Combining with nonlinear adaptive control [16], the unknown ship dynamics, environmental disturbances and measurement noise can be estimated. Combining with PD control [17], the proposed method can deal with abrupt disturbance like gust wind. Combining with genetic algorithm [18], the ANN structure and training cost are optimized and reduced, respectively, guaranteeing that the ship reach the dock smoothly. Apart from ANN, other methods, like adaptive backstepping control [19], PID-based nonlinear-feedback control [20], genetic algorithm-based optimal control [21], and PID-based active disturbance rejection control [22], provide solutions for self berthing aiming at handling wind loads.

Overall, self-berthing puts a high demand on the controller, requiring high control performance to force the ship stop at the exact place with a desired heading in the end. However, the real berthing situation at the end phase is a dynamic

Manuscript received February 3, 2021; accepted March 28, 2021. This work was supported by the China Scholarship Council (201806950080), the Researchlab Autonomous Shipping (RAS) of Delft University of Technology, and the INTERREG North Sea Region Grant "AVATAR" funded by the European Regional Development Fund. Recommended by Associate Editor Qing-Long Han. *(Corresponding author: Zhe Du.)*

Citation: Z. Du, R. R. Negenborn, and V. Reppa, "Cooperative multi-agent control for autonomous ship towing under environmental disturbances," *IEEE/CAA J. Autom. Sinica*, vol. 8, no. 8, pp. 1365–1379, Aug. 2021.

The authors are with the Department of Maritime and Transport Technology, Delft University of Technology, 2628 CD, Delft, The Netherlands (e-mail: Z.Du@tudelft.nl; R.R.Negenborn@tudelft.nl; V.Reppa@tudelft.nl).

Color versions of one or more of the figures in this paper are available online at http://ieeexplore.ieee.org.

Digital Object Identifier 10.1109/JAS.2021.1004078

Authorized licensed use limited to: TU Delft Library. Downloaded on March 04,2022 at 10:37:27 UTC from IEEE Xplore. Restrictions apply.

TABLE I
CLASSIFICATION OF AUTONOMOUS SHIP BERTHING, CORRESPONDING CONTROL METHODS, AND DISTURBANCE CONSIDERATIONS

Research article	Autonomous berthing way		Control method*									Disturbance model in control design
	Self-berthing	Assisted-berthing	ANN	MPC	AC	PID	GA	BS	OC	NC	FC	
[15]	✓		✓	✓								Wind
[16]	✓		✓		✓					✓		Bounded
[17]	✓		✓			✓						Wind
[18]	✓		✓				✓					Wind
[19]	✓				✓			✓				Wind
[20]	✓					✓				✓		Wind
[21]	✓						✓		✓			Wind
[22]	✓					✓				✓		Wind
[23]		Attaching								✓		Sinusoid-based
[24]		Attaching			✓				✓			Bounded
[25]		Attaching							✓			–
[26]		Pushing								✓		–
[27]		Pushing									✓	–
[28]		Towing						✓				–
[29]		Towing				✓						–
[30]		Towing							✓			–
[31]		Attaching & Towing		✓								–
This paper		**Towing**							✓			**Wind + Uncertainties**

* ANN: Artificial Neural Networks; MPC: Model Predictive Control; AC: Adaptive Control; PID: Proportional Integral Derivative; GA: Genetic Algorithm; BS: Backstepping; OC: Optimal Control; NC: Nonlinear Control; FC: Fuzzy Control.

process. On one hand, in the premise of under-actuated system, the low speed and the large size of the ship decrease the maneuverability dramatically. On the other hand, the environmental disturbances complicate significantly the control. Thus, the ship should adjust its states (position and heading) continuously to achieve the goal.

Assisted-berthing compensates the above limitation by transferring the high-demand control of one ship to the cooperative control of several autonomous tugs. In fact, this solution has gradually got attention since 2017 because some companies have launched projects to develop commercial autonomous vessels using tugboats [33]. According to their plans, tugboats will be one of the first vessel classes to become autonomous and the first step to "smart shipping". It is worth highlighting that autonomous tugboats does not exclude the involvement of human operators. This depends on the levels of autonomy [34].

Assisted-berthing is a multi-agent over-actuated control problem. There is no preferable control method in this field, but the way of manipulation plays a key role, categorized as: attaching, pushing, and towing. Attaching is the way that a swarm of autonomous tugs is fixed around the ship in such a way that the position and orientation of each tug to the ship-body frame do not change. The number of tugs should be even, usually four [25] or six [23], [24], to guarantee the connected system has a force equilibrium in the vertical direction. Before attaching, the tugs approach the object forming a proper configuration to prevent the object from escaping (form closure). After the connection, they are regarded as thrusters offering power to the object. Hence, the original problem is transformed into a control allocation problem [35]. This is an effective way, but the collision avoidance between the tugs and the ship and the design of the attached device are key points that may limit the applicability [36]. Most of the research works following the attaching approach assume that the tugs are connected to the object, and ignore the two issues.

Pushing is the way to control the tugs by keeping in touch with the ship without the tugs being fixed to one point. The number of the tugs is determined by satisfying the "conditional closure" (a term used in robotics, meaning that robots push an object on one side only [37]). This way is often applied to cooperative manipulation problems by mobile robots (box-pushing problems) because the direction and magnitude of the forces offered by robots do not require to be strictly controlled and the conditional closure increases the degree of freedom of the manipulation system [38]. This is a simple and direct way, but the application scenarios are limited to static environment. The disturbances of the sea environment (mainly the waves and current) increase the danger of the pushing process. Only a few research works propose this manipulation way [26], [27].

Towing is the way to manipulate the ship by using towlines that connect the ship and the tugs. The minimum number of tugs is two. Towing manipulation is widely used for ship assisting berthing in maritime practice, because it is well

Authorized licensed use limited to: TU Delft Library. Downloaded on March 04,2022 at 10:37:27 UTC from IEEE Xplore. Restrictions apply.

adapted not only in harsh weather and sea conditions but also in some restricted waters, like congested canals, narrow bridges and dry-docks [39]. Compared to attaching, the tug has no contact with the ship, minimizing the risk of collision during the connection process, and there is no need for additional devices besides the towing equipment that exists in every ship or platform like winches, hooks, bollards and towlines. Compared to pushing, it ensures a safe distance between the ASV and the ship, increasing the robustness to the dynamic sea condition and extreme weather disturbances. In the related research works [28]–[30], the authors pay attention to manipulate a ship or an unpowered facility following a predefined path (position control). However, for the ship berthing problem, guaranteeing the safety and efficiency of the manipulation process requires the additional control of the heading and velocity.

From the view of disturbance consideration, research works on self-berthing mainly take into account wind disturbances [15], [17]–[22]. Studies on assisted berthing have limited numbers, just some papers of using attaching manipulation way utilize functions to approximate the sea conditions, like sinusoid-based [23] and bounded functions [24].

B. Contributions

This paper focuses on cooperative control of multiple autonomous tugs for ship towing under environmental disturbances. A multi-layer multi-agent control architecture is proposed to solve the problem, where a control agent is designed for each tug and a supervisory controller is used to coordinate the control agents. The main contributions of this research work are:

1) The proposed control scheme is designed not only to transport the ship to a desired position but also to regulate its heading and speed. The multi-layer control architecture offers the flexibility in performing different control tasks to coordinate multiple autonomous tugs.

2) Derivation of the kinematic model of the physically interconnected ship-towing system links the higher layer and lower layer controller. The desired towing forces and angles calculated by the higher layer (supervisory) controller are utilized through this kinematic model to compute the desired trajectories of the tugs, providing the on-line tracking reference for the lower layer (tug) controllers.

3) Considering the main influence of the wind, an adaptive weight coefficient matrix is designed. The matrix is time-varying according to the current ship states so that it can adjust the proportion of the penalty between position errors and velocity errors applied in optimal control strategy. This property is useful to force the ship to the desired states (especially for heading) in (hard) wind disturbances. Moreover, by tuning the matrix, the velocity of the ship through the whole towing process can be increased reducing the time cost.

In this paper, scaled models are considered because models for these are available (details are seen in Section IV), without loss of generality. Preliminary results of this work obtained assuming no disturbances are presented in [40]. Compared to [40], the proposed control scheme is designed to cope with environmental disturbances. Extensive simulations have been carried out to show the robustness of the proposed method in scenarios with various environmental disturbances in a realistic framework.

C. Outline

This paper is organized as follows. In Section II, the problem is described and transformed into the mathematical model. The design of the multi-layer multi-agent control algorithm is given in Section III. The results of simulation experiments are provided in Section IV to demonstrate the effectiveness of the proposed algorithm applied to a ship towing system with small-scale vessels, followed by the analysis and explanation. Finally, the conclusions and future research directions are given in Section V.

II. Problem Statement

The plane motion of a vessel can be described by the 3-DOF (degree of freedom) kinematics and kinetics model, which is expressed as [41]

$$\begin{aligned}\dot{\boldsymbol{\eta}}(t) &= \boldsymbol{R}(\psi(t))\boldsymbol{\nu}(t)\\ \boldsymbol{M}\dot{\boldsymbol{\nu}}(t) + \boldsymbol{C}(\boldsymbol{\nu}(t))\boldsymbol{\nu}(t) + \boldsymbol{D}\boldsymbol{\nu}(t) &= \boldsymbol{\tau}(t) + \boldsymbol{\tau}_e(t)\end{aligned} \tag{1}$$

where $\boldsymbol{\eta}(t) = [x(t)\ \ y(t)\ \ \psi(t)]^T \in \mathbb{R}^3$ is the position vector in the world frame (North-East-Down) including position coordinates $(x(t),\ y(t))$ and heading $\psi(t)$; $\boldsymbol{\nu}(t) = [u(t)\ \ v(t)\ \ r(t)]^T \in \mathbb{R}^3$ is the velocity vector in the Body-fixed frame containing the velocity of surge $u(t)$, sway $v(t)$, and yaw $r(t)$; $\boldsymbol{R} \in \mathbb{R}^{3\times3}$ is the rotation matrix from the body frame to the world frame, which is a function of heading

$$\boldsymbol{R}(\psi(t)) = \begin{bmatrix} \cos(\psi(t)) & -\sin(\psi(t)) & 0 \\ \sin(\psi(t)) & \cos(\psi(t)) & 0 \\ 0 & 0 & 1 \end{bmatrix}. \tag{2}$$

The terms $\boldsymbol{M} \in \mathbb{R}^{3\times3}$, $\boldsymbol{C} \in \mathbb{R}^{3\times3}$, and $\boldsymbol{D} \in \mathbb{R}^{3\times3}$ are the Mass (inertia), Coriolis-Centripetal, and Damping matrix, respectively. The first two matrices include rigid-body and added mass parts, and the last matrix is only considered to have a linear part. The variable $\boldsymbol{\tau}(t) = [\tau_u(t)\ \ \tau_v(t)\ \ \tau_r(t)]^T \in \mathbb{R}^3$ is the controllable input referring to the forces $\tau_u(t)$, $\tau_v(t)$, and moment $\tau_r(t)$, while $\boldsymbol{\tau}_e(t) \in \mathbb{R}^3$ stands for the environmental disturbance forces and moment.

A. Controllable Input of the Vessels

In this work, we assume that the ship cannot move by itself. The power that moves the ship is offered by the forces through the towlines applied by the tugs. Thus, the controllable input of the ship $\boldsymbol{\tau}_S(t)$ (in (1) $\boldsymbol{\tau}(t) \triangleq \boldsymbol{\tau}_S(t)$) can be expressed as

$$\begin{aligned}\boldsymbol{\tau}_S(t) &= \sum_{i=1}^{n} [\boldsymbol{\tau}_{S_i}(t)]\\ &= \sum_{i=1}^{n} [\boldsymbol{L}_{S_i}(l_{x_i}, l_{y_i})\boldsymbol{B}_{S_i}(\alpha_i(t))F_i(t)]\end{aligned}$$

Authorized licensed use limited to: TU Delft Library. Downloaded on March 04,2022 at 10:37:27 UTC from IEEE Xplore. Restrictions apply.

$$\boldsymbol{L}_{S_i} = \begin{bmatrix} 1 & 0 \\ 0 & 1 \\ l_{x_i} & l_{y_i} \end{bmatrix}$$

$$\boldsymbol{B}_{S_i} = \begin{bmatrix} \cos(\alpha_i(t)) \\ \sin(\alpha_i(t)) \end{bmatrix} \tag{3}$$

where n is the number of tugs; $\boldsymbol{\tau}_{S_i}(t)$ represents the towing forces and moment by Tug i; $\boldsymbol{L}_{S_i} \in \mathbb{R}^{3\times 2}$ is the force arm matrix with respect to the ship-body frame, which is a function of the longitudinal (l_{x_i}) and lateral (l_{y_i}) distance from the towing point to the centre of gravity of the ship (shown in Fig. 1(a)); $\boldsymbol{B}_{S_i} \in \mathbb{R}^{2\times 1}$ is the configuration matrix with respect to the ship-body frame, which is a function of the towing angle $\alpha_i(t)$. The variable $F_i(t)$ is the towing force generated from the tug i through the towline with no force loss.

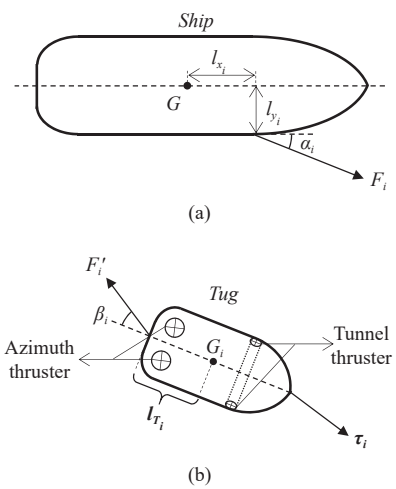

Fig. 1. Physical schematic diagrams: (a) Ship; (b) Tug.

In order to meet the flexibility in ship assisted berthing, the actuator system of the tug generally contains two stern azimuth thrusters and one bow tunnel thruster (as shown in Fig. 1(b)), known as the *ASD tug* [39]. With the help of three thrusters, the tug can obtain omnidirectional forces and moments. The controllable input $\boldsymbol{\tau}_i(t) \in \mathbb{R}^3$ from the thrusters of tug i can be expressed as

$$\boldsymbol{\tau}_i(t) = \boldsymbol{\tau}_{T_i}(t) + \boldsymbol{\tau}_{F_i}(t) \tag{4}$$

where $\boldsymbol{\tau}_{T_i}(t) \in \mathbb{R}^3$ denotes the forces and moment to move the tug; $\boldsymbol{\tau}_{F_i}(t) \in \mathbb{R}^3$ represents the forces and moment to compensate for the reaction of towing force, which can be expressed as

$$\boldsymbol{\tau}_{F_i}(t) = \boldsymbol{L}_{T_i}(l_{T_i})\boldsymbol{B}_{T_i}(\beta_i(t))F_i'(t)$$

$$\boldsymbol{L}_{T_i} = \begin{bmatrix} 1 & 0 \\ 0 & 1 \\ 0 & l_{T_i} \end{bmatrix}$$

$$\boldsymbol{B}_{T_i} = \begin{bmatrix} \cos(\beta_i(t)) \\ \sin(\beta_i(t)) \end{bmatrix} \tag{5}$$

where $\boldsymbol{L}_{T_i} \in \mathbb{R}^{3\times 2}$ is the force arm matrix with respect to the tug-body frame, which is a function of the distance from the towing point on tug to the centre of gravity of the tug (l_{T_i}, shown in Fig. 1(b)); $\boldsymbol{B}_{T_i} \in \mathbb{R}^{2\times 1}$ is the configuration matrix with respect to the tug-body frame, which is a function of the tug angle $\beta_i(t)$; $F_i'(t)$ is the force applied through a controlled winch onboard the tugboat to the towline, $F_i'(t) = F_i(t)$. In this work, we do not consider the low-level winch control and the detailed model of the force F_i as a function of the elastic elongation and the generalized stiffness that depends on the material, diameter and the strand construction of the towline.

The interconnection between the ship system and the tug system is the towing force $F_i(t)$. For the ship, the towing force provides power to move it, while for tugs, the towing force is the resistance effect which needs to be compensated.

B. Environmental Disturbances

In this work we consider that the operation of ship berthing happens near the port areas, implying that the wind force is dominant [42]. Thus, the environmental disturbances are divided into the wind effects $\boldsymbol{\tau}_w(t) \in \mathbb{R}^3$ and the other unknown effects $\boldsymbol{\tau}_{cw}(t) \in \mathbb{R}^3$ (mainly refer to waves and currents)

$$\boldsymbol{\tau}_e(t) = \boldsymbol{\tau}_w(t) + \boldsymbol{\tau}_{cw}(t). \tag{6}$$

The unknown part is difficult to be measured in real-time and characterized as stochastic, an approximated model will be illustrated in Section IV. On the contrary, the wind speed denoted by $V_w(t)$ and wind direction denoted by $\beta_w(t)$ can be easily measured by an anemometer and a weather vane in real-time, respectively. The effects of wind disturbances on a vessel (under velocity $u(t)$, $v(t)$, and heading $\psi(t)$), which are considered symmetrical with respect to the xz and yz planes can be expressed by [41]

$$\boldsymbol{\tau}_w(t) = \frac{1}{2}\rho_a V_{rw}^2(t) \begin{bmatrix} -c_x\cos(\gamma_{rw}(t))A_{Fw} \\ c_y\sin(\gamma_{rw}(t))A_{Lw} \\ c_n\sin(2\gamma_{rw}(t))A_{Lw}L_{oa} \end{bmatrix} \tag{7}$$

$$\begin{aligned} V_{rw}(t) &= \sqrt{u_{rw}{}^2(t) + v_{rw}{}^2(t)} \\ \gamma_{rw}(t) &= \operatorname{atan2}(v_{rw}(t), u_{rw}(t)) \\ u_{rw}(t) &= u(t) - u_w(t) \\ v_{rw}(t) &= v(t) - v_w(t) \\ u_w(t) &= V_w(t)\cos(\beta_w(t) - \psi(t)) \\ v_w(t) &= V_w(t)\sin(\beta_w(t) - \psi(t)) \end{aligned} \tag{8}$$

where ρ_a is the air density; c_x, c_y, and c_n are the wind coefficients for horizontal plane motions; A_{Fw} and A_{Lw} are the transverse and lateral projected area of vessel above the water, respectively; L_{oa} is the overall length of vessel; $V_{rw}(t)$ and $\gamma_{rw}(t)$ are the relative wind speed and the wind angle of attack relative to the vessel bow, respectively; $u_{rw}(t)$ and $v_{rw}(t)$ are the relative wind speed in the x and y directions (vessel body frame), respectively; $u_w(t)$ and $v_w(t)$ are the components of wind speed $V_w(t)$ in the x and y directions (world frame).

C. Towing System and Control Objective

Without loss of generality, we consider a towing system that

Authorized licensed use limited to: TU Delft Library. Downloaded on March 04,2022 at 10:37:27 UTC from IEEE Xplore. Restrictions apply.

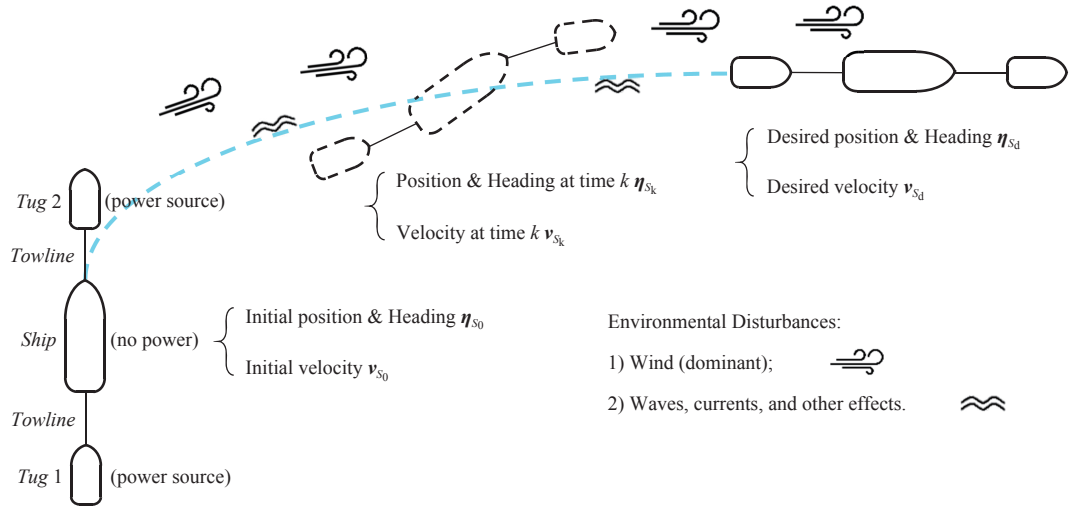

Fig. 2. Typical towing system and control objective.

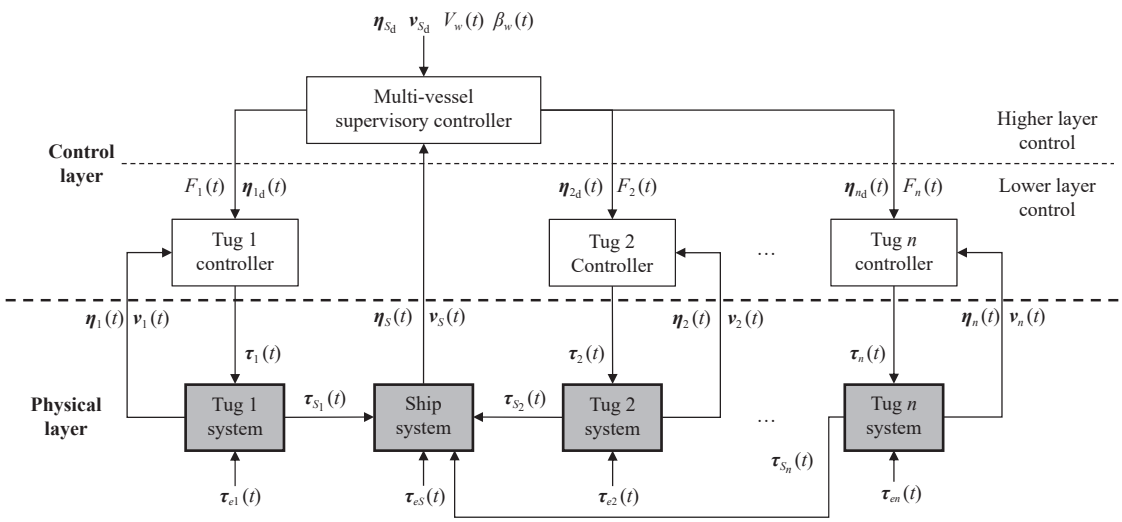

Fig. 3. Control diagram for the multi-vessel towing system.

consists of one ship and two tugs as shown in Fig. 2, where the two tugs have enough power to perform the towing process. The ship is assumed to have no power and the power sources (control inputs) of the system are offered by the two tugs. The front tug (Tug 2) is to increase the ship speed and alter the heading, the aft tug (Tug 1) is to decrease the ship speed and stabilize the course. The control objective is to move the ship from the initial states ($\boldsymbol{\eta}_{S_0}$, $\boldsymbol{v}_{S_0}$) to the desired states ($\boldsymbol{\eta}_{S_d}, \boldsymbol{v}_{S_d}$). In the towing process, the whole system is influenced by the environmental disturbances, which include the dominant effect of wind and the unknown other effects.

III. Multi-Agent, Multi-Layer Control Scheme

According to the characteristics of the towing system and the control objective, a multi-layer control architecture is used, which has advantages of performing different control tasks to coordinate multiple agents [8]. Comparing with the single layer, in the multi-layer control architecture, a higher layer considers a larger part of the system and can therefore direct the lower control layer to achieve coordination [43].

As shown in Fig. 3, the physical layer in the bottom contains all the physical system components, including hulls, actuators (thrusters), towlines, sensors, etc. The ship is manipulated by n tugs through towline which transfer towing forces and moment ($\boldsymbol{\tau}_{S_i}(t)$). All the physical systems are affected by the environmental disturbances ($\boldsymbol{\tau}_{eS}(t)$ and $\boldsymbol{\tau}_{ei}(t)$).

The control layer is distributed in two sublayers: higher-layer control and lower-layer control. The higher-layer control objective is to coordinate the two tugs by allocating the tasks. Comparing the goal ($\boldsymbol{\eta}_{S_d}, \boldsymbol{v}_{S_d}$) and current ($\boldsymbol{\eta}_S(t), \boldsymbol{v}_S(t)$) states of the ship and acquiring the wind information ($V_w(t)$, $\beta_w(t)$), the supervisory controller generates the online desired trajectories ($\boldsymbol{\eta}_{i_d}(t)$) for tugs. The lower-layer control objective is to execute the tasks allocated by the higher-layer control that makes each tug track its trajectory reference. Based on the tug reference trajectories ($\boldsymbol{\eta}_{i_d}(t)$) and current tug states ($\boldsymbol{\eta}_i(t), \boldsymbol{v}_i(t)$), the tug controllers calculate the forces and moment that the thrusters should provide ($\boldsymbol{\tau}_i(t)$).

A. Supervisory Controller

The inner structure of the supervisory controller is shown in Fig. 4. There are three core components: Optimizer, Adaptive

Authorized licensed use limited to: TU Delft Library. Downloaded on March 04,2022 at 10:37:27 UTC from IEEE Xplore. Restrictions apply.

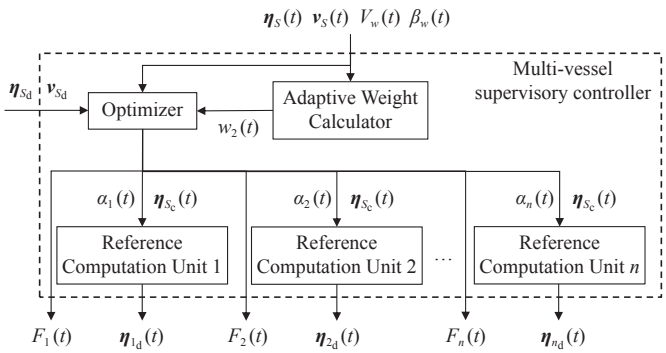

Fig. 4. Inner structure of the multi-vessel supervisory controller.

Weight Calculator, and Reference Computation Unit.

1) Optimizer: The objective of the optimizer is to compute the towing forces and angles. Due to multiple variables (towing forces and angles) that need to be determined, the optimal control method [44] is used to obtain a rational combination solving of these variables. Thus, the problem can be expressed as finding $\alpha_i(t)$ and $F_i(t)$ to minimize the cost function

$$\begin{aligned} J_S(t) &= \boldsymbol{e}_{S_\eta}^T(t) w_1(t) \boldsymbol{e}_{S_\eta}(t) + \boldsymbol{e}_{S_v}^T(t) w_2(t) \boldsymbol{e}_{S_v}(t) \\ \boldsymbol{e}_{S_\eta}(t) &= \boldsymbol{\eta}_{S_C}(t) - \boldsymbol{\eta}_{S_d} \\ \boldsymbol{e}_{S_v}(t) &= \boldsymbol{v}_{S_C}(t) - \boldsymbol{v}_{S_d} \end{aligned} \tag{9}$$

where $\boldsymbol{e}_{S_\eta}(t) \in \mathbb{R}^3$ and $\boldsymbol{e}_{S_v}(t) \in \mathbb{R}^3$ are the position and velocity error, respectively; $w_1(t)$ and $w_2(t)$ are the adaptive weights defined in the next subsection, whose values are related to the current measured wind data and ship states; $\boldsymbol{\eta}_{S_C}(t) \in \mathbb{R}^3$ and $\boldsymbol{v}_{S_C}(t) \in \mathbb{R}^3$ are the calculated predicted ship position and velocity, which subject to the ship dynamics constraint ((1)–(3) and (6)–(8), where the unknown part of the environmental disturbances $\boldsymbol{\tau}_{cw}$ in (6) is not taken into consideration) that is a function of $\alpha_i(t)$ and $F_i(t)$.

Remark (Realization of $F_i(t)$): $F_i(t)$ can be realized by the winch on the tugboat in practical. The winch is considered to be controlled by another controller, which is out of the scope of this work.

According to the physical law and tug practical operation [39], the towing forces and angles have to satisfy the following saturation constraints:

$$\begin{aligned} &\alpha_i(t) \in [-45°, 45°] \\ &F_i(t) \in [0, F_{i\max}] \quad (i = 1, 2) \end{aligned} \tag{10}$$

where $F_{i\max}$ is the maximum value of towing force that the two towlines withstand.

Furthermore, the performance of the trajectory tracking in the lower-layer is related to the quality of the tug reference trajectory, which is affected by the change rate of the towing angles and forces. Thus, a saturation constraint of the change rate for the two towing angles and forces is set to make the reference trajectory smooth

$$\begin{aligned} &|\dot{\alpha}_i(t)| \le \bar{\alpha}_i \\ &\left|\dot{F}_i(t)\right| \le \bar{F}_i \quad (i = 1, 2) \end{aligned} \tag{11}$$

where $\bar{\alpha}_i$ and $\bar{F}_i$ are the maximum change rate value of towing angle and force, respectively.

2) Adaptive Weight Calculator: The two weight coefficients $(w_1(t), w_2(t))$ in the cost function (9) determine which part (position or velocity) the controller puts more efforts to regulate. If $w_1(t) >> w_2(t)$, the controller puts more effort into the ship position and the towing process is fast, but the towing trajectory is not smooth because of the large fluctuated velocity. In contrast, if $w_1(t) << w_2(t)$, the controller concentrates on regulating the ship velocity leading to a smoother trajectory, but the time of the whole process is much longer delaying other ship operations. Thus, the appropriate selection of the weight proportion plays an important role in the supervisory controller. To design adaptive weights, the following requirements should be taken into consideration.

i) Requirement 1: Stable at the beginning

At the beginning of the towing, the task for the two autonomous tugs is to adjust themselves to a proper configuration to manipulate the ship. To stabilize the towing system, the velocity in this phase should be low with minimum fluctuation. Thus, the controller should focus on regulating the ship velocity.

ii) Requirement 2: Reach the goal in the end

At the end phase of the towing, as the towing system approaching the goal, the velocity asymptotically goes to zero. The task at this moment is to make sure the ship reaches the desired position with the desired heading. Thus, the controller should decrease the ship velocity and accelerate the regulation of ship position.

iii) Requirement 3: Robust to the wind

Due to the influence of the wind disturbances, it is difficult to stabilize the motion of the towing system at the beginning and the goal of the ship, especially the heading, is more difficult to achieve at the end phase. Thus, the controller should put more effort into satisfying the Requirements 1 and 2 according to the wind strength (V_w), and should prioritize the heading control.

iv) Requirement 4: Reduce control input oscillation

Control input oscillation determines the practicality of the proposed approach. A practical control approach should have less oscillation of the control input. Thus, at the end phase of the towing, the value of the weight should be designed as constant; in other phases, the changes in the weight should be smooth and not too much.

Based on the above requirements, the position weight is set as $w_1(t) = \mathrm{diag}(1, 1, 1)$, while the adaptive velocity weight $w_2(t) = \mathrm{diag}(w_u(t), w_v(t), w_r(t))$ is designed as

$$\begin{aligned} w_u(t) &= w_v(t) = w_r(t) = k_0(1 + V_w(t))(d(t)/d_0) \\ d_0 &= \sqrt{(x_{S_d} - x_{S_0})^2 + (y_{S_d} - y_{S_0})^2} \\ d(t) &= \sqrt{(x_{S_d} - x_S(t))^2 + (y_{S_d} - y_S(t))^2} \end{aligned} \tag{12}$$

whose terminal values $w_{2t}(t) = \mathrm{diag}(w_{ut}(t), w_{vt}(t), w_{rt}(t))$ are set as

$$\begin{aligned} w_{ut}(t) &= w_{vt}(t) = k_t[1 - V_w(t)/(V_w(t) + k_1)] \\ w_{rt}(t) &= k_t[1 - V_w(t)/(V_w(t) + k_2)] \end{aligned} \tag{13}$$

Authorized licensed use limited to: TU Delft Library. Downloaded on March 04,2022 at 10:37:27 UTC from IEEE Xplore. Restrictions apply.

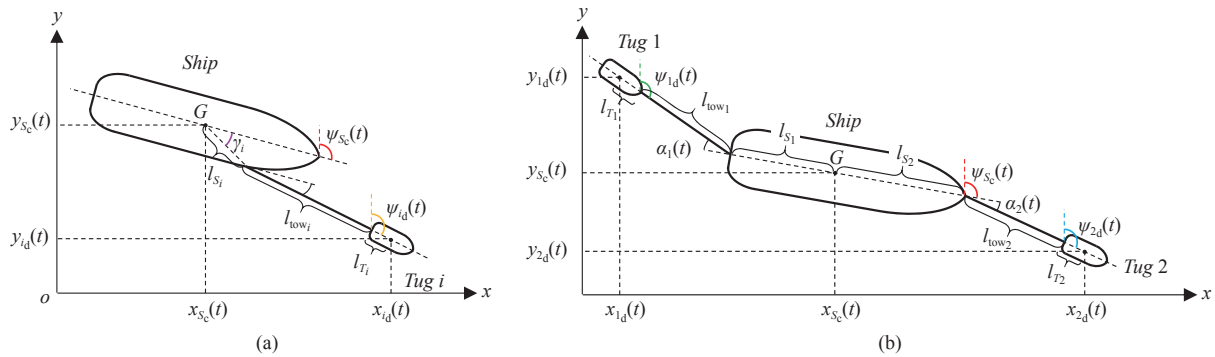

Fig. 5. Geometrical kinematics of the ship towing system relation diagram: (a) General case; (b) Case in this paper.

where d_0 is the distance from the origin (x_{S_0}, y_{S_0}) to the destination (x_{S_d}, y_{S_d}); $d(t)$ is the distance from the current ship position $(x_S(t), y_S(t))$ to the destination, which is the position error. k_0, k_t, k_1, and k_2 are the positive coefficients: k_0 and k_t determine the initial and final value of the weight, so $k_0 > k_t > 1$; k_1 and k_2 define the final values of the linear and angular velocity weight, they are set to be $0 < k_2 < k_1 < 1$ to emphasize the heading control at the end phase.

As the value of $d(t)$ decreases over the process of towing, the adaptive weight $w_2(t)$ is decreasing according to (12). When the ship is so close to the destination that the adaptive weight value is smaller than the terminal setting in (13), the adaptive weight will be fixed on the terminal value.

3) Reference Computation Unit: The Reference Computation Unit (see Fig. 3) aims to calculate the desired position and heading of the tug in order to tow the ship. The computation is realized based on the desired geometry relationship between the ship and tug. Once the towing forces and angles for the ship are provided by the higher layer control, the position and heading of the ship are determined. As shown in Fig. 5(a), the desired position and heading of tug i can be calculated by the determined ship position and heading

$$\begin{aligned}\boldsymbol{\eta}_{i\mathrm{d}}(t) &= \boldsymbol{\eta}_{S_\mathrm{C}}(t) + (l_{\mathrm{tow}_i} + l_{T_i})\boldsymbol{E}_i(\psi_{S_\mathrm{C}}(t), \alpha_i(t)) \\ &\quad + l_{S_i}\boldsymbol{F}_i(\psi_{S_\mathrm{C}}(t), \gamma_i) + \alpha_i(t)[0\ 0\ 1]^T \end{aligned} \tag{14}$$

where l_{tow_i} is the desired elongation of the towline that guarantees the action of the restoring force and the collision avoidance between the two vessels; l_{S_i} the distance from the centre of gravity of the ship (G) to the towing point; γ_i is the angle between the heading of the ship and the direction from G to the towing point; $\boldsymbol{E}_i \in \mathbb{R}^3$ and $\boldsymbol{F}_i \in \mathbb{R}^3$ are the vectors related to the predicted heading of the ship and the towing angles, formulated as

$$\boldsymbol{E}_i = (-1)^{m_i}\begin{bmatrix} \sin(\psi_{S_\mathrm{C}}(t) + \alpha_i(t)) \\ \cos(\psi_{S_\mathrm{C}}(t) + \alpha_i(t)) \\ 0 \end{bmatrix} \tag{15}$$

$$\boldsymbol{F}_i = (-1)^{m_i}\begin{bmatrix} \sin(\psi_{S_\mathrm{C}} + \gamma_i) \\ \cos(\psi_{S_\mathrm{C}} + \gamma_i) \\ 0 \end{bmatrix} \tag{16}$$

where $m_i = 0$ when tug i is located in front of the centre of gravity of the ship (G), $m_i = 1$ when tug i is located behind the centre of gravity of the ship (G).

For the case in this paper, the geometrical kinematics of one ship and two tugs are shown in Fig. 5(b). It can be seen that $\gamma_1 = 0$, $\gamma_2 = 0$, $m_1 = 1$, $m_2 = 0$, so the corresponding $\boldsymbol{E}_1$, $\boldsymbol{F}_1$ and $\boldsymbol{E}_2$, $\boldsymbol{F}_2$ are

$$\boldsymbol{E}_1 = -\begin{bmatrix} \sin(\psi_{S_\mathrm{C}}(t) + \alpha_1(t)) \\ \cos(\psi_{S_\mathrm{C}}(t) + \alpha_1(t)) \\ 0 \end{bmatrix} \boldsymbol{F}_1 = -\begin{bmatrix} \sin(\psi_{S_\mathrm{C}}(t)) \\ \cos(\psi_{S_\mathrm{C}}(t)) \\ 0 \end{bmatrix} \tag{17}$$

$$\boldsymbol{E}_2 = \begin{bmatrix} \sin(\psi_{S_\mathrm{C}}(t) + \alpha_2(t)) \\ \cos(\psi_{S_\mathrm{C}}(t) + \alpha_2(t)) \\ 0 \end{bmatrix} \boldsymbol{F}_2 = \begin{bmatrix} \sin(\psi_{S_\mathrm{C}}(t)) \\ \cos(\psi_{S_\mathrm{C}}(t)) \\ 0 \end{bmatrix}. \tag{18}$$

Thus, the algorithm flow in the higher layer control is summarized in Algorithm 1:

Algorithm 1 Higher Layer Control

Input: Desired ship position and velocity $\boldsymbol{\eta}_{S_\mathrm{d}}$, $\boldsymbol{\nu}_{S_\mathrm{d}}$; Current ship position and velocity $\boldsymbol{\eta}_S(t)$, $\boldsymbol{\nu}_S(t)$; Wind speed and angle $V_w(t)$, $\beta_w(t)$.

Step 1: Calculate current adaptive velocity weight $w_2(t)$ according to (12) and the corresponding terminal value according to (13). If $w_2(t) > w_t(t)$, then take $w_2(t)$ as the current adaptive weight; otherwise, take $w_t(t)$ as the current adaptive weight.

Step 2: Compute towing forces F_i and angles α_i according to the cost function (9), restricted by the ship dynamics (1)–(3), the environmental disturbances (6)–(8), and the control constraints (10) and (11).

Step 3: Calculate the tug reference trajectory $\boldsymbol{\eta}_{i\mathrm{d}}(t)$ according to (14)–(16).

Output: Towing forces $F_i(t)$ and Tug reference trajectory $\boldsymbol{\eta}_{i\mathrm{d}}(t)$.

B. Tug Controller

The objective of the Tug Controller is to determine the thruster forces and moment to track the reference trajectories $(\boldsymbol{\eta}_{i_\mathrm{d}}(t))$. The problem can be expressed as finding $\boldsymbol{\tau}_i(t)$ for Tug i to minimize the cost function

$$\begin{aligned} J_i(t) &= \boldsymbol{e}_{i_\eta}^T(t)\boldsymbol{e}_{i_\eta}(t) \\ \boldsymbol{e}_{i_\eta}(t+1) &= \boldsymbol{\eta}_{i_\mathrm{C}}(t) - \boldsymbol{\eta}_{i_\mathrm{d}}(t) \end{aligned} \tag{19}$$

where $\boldsymbol{e}_{i_\eta}(t) \in \mathbb{R}^3$ is the position error; $\boldsymbol{\eta}_{i_\mathrm{C}}(t) \in \mathbb{R}^3$ is the calculated predicted tug position vector, which is subject to

Authorized licensed use limited to: TU Delft Library. Downloaded on March 04,2022 at 10:37:27 UTC from IEEE Xplore. Restrictions apply.

the tug dynamics constraint ((1), (2), (4), and (5), whose unknown part of the environmental disturbances $\boldsymbol{\tau}_{cw}$ in (6) is not taken into consideration) that is a function of $\boldsymbol{\tau}_i(t)$.

According to the relationship among the tug angle β_i, desired tug heading ψ_{i_d} and actual tug heading ψ_i (shown in Fig. 6), the tug angle can be expressed as

$$\beta_i = \psi_{i_\mathrm{d}} - \psi_i \tag{20}$$

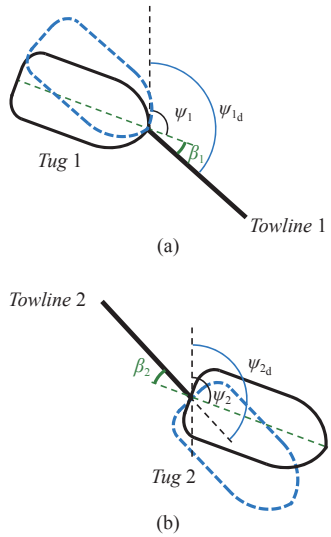

Fig. 6. Relationship among tug angle β_i, desired tug heading ψ_{i_d} and actual tug heading ψ_i: (a) Tug 1; (b) Tug 2.

The forces and moment of the thrusters satisfy the saturation constraints

$$\boldsymbol{\tau}_i \in [-\boldsymbol{\tau}_{i\max}, \boldsymbol{\tau}_{i\max}] \qquad (i = 1, 2) \tag{21}$$

where $\boldsymbol{\tau}_{i\max}$ is the maximum value of the thruster forces and moment.

The main process steps of the lower layer control are summarized in Algorithm 2.

Algorithm 2 Lower Layer Control

Input: Tug reference trajectory $\boldsymbol{\eta}_{i\mathrm{d}}(t)$; Towing forces F_i; Current tug position and velocity $\boldsymbol{\eta}_i(t)$, $\boldsymbol{\nu}_i(t)$; Wind speed and angle $V_w(t)$, $\beta_w(t)$.

Step 1: Compute tug thruster forces and moment $\boldsymbol{\tau}_i(t)$ according to the cost function (19) and the tug angle (20), restricted by the tug dynamics (1), (2) and (4), (5), the environmental disturbances (6)–(8), and the control constraints (21).

Output: Tug thruster forces and moment $\boldsymbol{\tau}_i(t)$.

IV. Simulation and Discussion

In this section, simulation results are presented to show the performance of the proposed control algorithm applied to scaled vessel models, followed by the discussion and analysis of the results.

The two tugs are modelled based on the "*TitoNeri*", which is developed by TU Delft [45]. The ship model considered is the "*CyberShip II*", which has been developed by NTNU [46]. The design information for "*TitoNeri*" and "*CyberShip II*" is given in Table II , while the parameters and the physical constraints of the towing system are shown in Table III.

The environmental disturbances are simulated based on information provided by the port of Rotterdam [47]. According to its latest meteorological information, 98% of the wind effects are not greater than 7 Beaufort (the wind speed is between 13.9 m/s and 17.1 m/s). According to Froude's scaling law [48], the scaled velocity is determined by the square root of the scaling factor (k). Since the scaling factor of the "*CyberShip II*" is 70 [46], the scaled wind speed can be expressed as

$$V_w' = V_w / \sqrt{70} \tag{22}$$

and the maximum value of the scaled wind speed is $17.1\ \mathrm{m/s} \div \sqrt{70} = 2\ \mathrm{m/s}$.

The adaptive weights of the supervisory controller given in (12) and (13) are selected as $k_0 = 150$, $k_t = 50$, $k_1 = 0.15$, $k_2 = 0.01$.

The unknown disturbances (mainly refer to waves) are considered to have less effect than the wind. Since the trigonometric function can be used to approximate the spectrum of the waves, many ship motion control-related research works describe the unknown disturbances using sinusoidal function adding constant [49]–[52] or random parts $(A\sin(\omega_1 t) + B \times \mathrm{rand}(t))$ [53], [54]. However, for the environment near ports (windy but sheltered areas), the wave period is short [39] $(A\sin(\omega_2 t) + B \times \mathrm{rand}(t),\ \ \omega_2 > \omega_1)$. Compared to the function image of a random function adding a constant $(C \times \mathrm{rand}(t) + D)$, if the wave period is short enough, the two approximated ways are similar. In practice, the information of the wave height, period and length are difficult to be measured accurately and timely. In contrast, according to the above analysis, the simpler way can reflect both the short period wave character and randomness. Thus, the unknown disturbances can be described by a random function plus a constant.

From the meteorological point of view, waves and currents are generated by wind [55], which means their effects are related to the wind speed $V_w(t)$ and direction $\beta_w(t)$. Therefore, the unknown disturbances in this paper are expressed as

$$\boldsymbol{\tau}_{cw} = \begin{bmatrix} k_X V_w(t)(\mathrm{rand}(t) + a_X)\cos(\beta_w(t) - \psi) A_{FD} \\ k_Y V_w(t)(\mathrm{rand}(t) + a_Y)\sin(\beta_w(t) - \psi) A_{LD} \\ k_N V_w(t)(\mathrm{rand}(t) + a_N)\cos(\beta_w(t) - \psi) A_{LD} L_{oa} \end{bmatrix} \tag{23}$$

where k_X, k_Y, and k_N are the unknown disturbance gain, whose values are less than 0.1; rand(t) is the random function from 0 to 1; a_X, a_Y, and a_N are the disturbance constant, whose values are less than 1; A_{FD} and A_{LD} are the transverse and lateral projected area of vessel under the water, respectively; ψ is the vessel's heading. In this simulation, the gains and constants are chosen as $k_X = 0.008$, $k_Y = 0.01$, $k_N = 0.0016$; $a_X = a_Y = a_N = 0.75$.

The initial position of the ship is located at the origin with zero degree of heading and no speed. The coordinates of the desired position are $(x_{S_\mathrm{d}}, y_{S_\mathrm{d}}) = (40, 25)$, and the desired heading is $\psi_{S_\mathrm{d}} = 90°$ with no speed. We perform two simulation scenarios, with and without environmental

Authorized licensed use limited to: TU Delft Library. Downloaded on March 04,2022 at 10:37:27 UTC from IEEE Xplore. Restrictions apply.

TABLE II
DESIGN INFORMATION OF "*CYBERSHIP II*" AND "*TITONERI*"

Vessel	Length (m)	Width (m)	Mass (kg)	Actuators	Physical Picture
TitoNeri	0.97	0.30	16.9	1) Two stern azimuth thrusters 2) One bow thruster	
CyberShip II	1.255	0.29	23.8	1) Two stern propellers with two rudders 2) One bow thruster	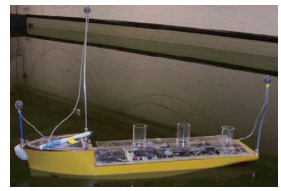

TABLE III
PARAMETERS OF THE TOWING SYSTEM

Desired elongation of towline	$l_{\text{tow}_1} = 1$ m	$l_{\text{tow}_2} = 1$ m
Distance from the ship centers of gravity	$l_{S_1} = 0.67$ m	$l_{S_2} = 0.585$ m
Distance from the tug centers of gravity	$l_{T_1} = 0.5$ m	$l_{T_2} = 0.5$ m
Maximum values of the towing forces	$F_{1\max} = 3$ N	$F_{2\max} = 3$ N
Maximum values of the thruster forces	$\tau_{1\max} = 10$ N	$\tau_{2\max} = 10$ N
Maximum rate of change of towing angles	$\bar{\alpha}_1 = 5\,°/\text{s}$	$\bar{\alpha}_2 = 5\,°/\text{s}$
Maximum rate of change of towing forces	$\bar{F}_1 = 0.1$ N/s	$\bar{F}_2 = 0.1$ N/s

disturbances, to compare the performance of the proposed multi-layer, multi-agent control architecture using constant and adaptive weights. Thus, two control schemes are designed: in the (A)-scheme, the supervisory controller uses constant weights with $w_2(t) = \text{diag}(150, 150, 150)$; in the (B)-scheme, the supervisory controller uses $w_2(t)$ defined through (12) and (13), the corresponding coefficients are set as $k_0 = 150$, $k_t = 50$, $k_1 = 0.15$, $k_2 = 0.01$.

A. Simulation Without Disturbances

When there are no disturbances, the ship towing process using the (A) and (B) control schemes are shown in Fig. 7. The two tugs cooperate to transport the ship to the goal position with the desired heading, but the time cost is different. In the first two sample times, the two control schemes have the same pace. At time $t_3 = 50$ s, the Tug 2 (blue) in Fig. 7(b) has already a horizontal displacement of 10 m, while it does not reach in Fig. 7(a). After t_3, the average speed of the towing system controlled by scheme B is higher than scheme A, so the time cost by scheme B is less than scheme A. From the character of the system position under the nine sampled times, Fig. 7(a) shows the average distribution due to the constant velocity weight, while Fig. 7(b) is charactered dense in the beginning and end, sparse in the middle phase. This results from that the adaptive velocity weights (12) decrease as the towing system approaches the destination, the speed of the system increases. When the weights reach their terminal value they are constant, and the speed of the system decrease.

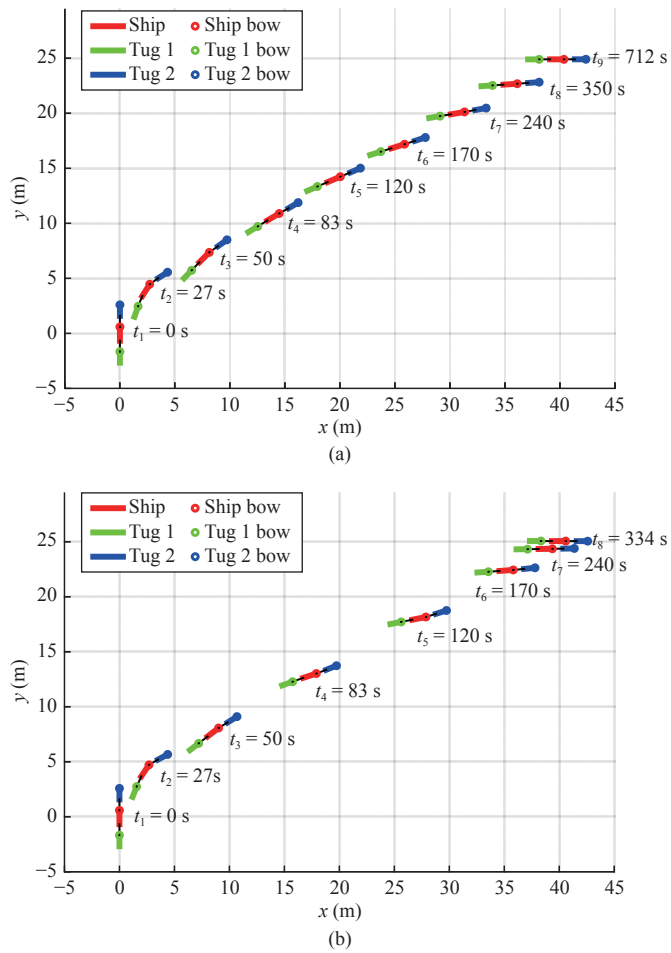

Fig. 7. Ship towing process without disturbances: (a) (A)-control scheme; (b) (B)-control scheme.

The states of the ship and two tugs are illustrated in Figs. 8 and 9, respectively. From Fig. 8, the velocities of the ship controlled by the two algorithms both converge to 0. The difference is that the peak value of the velocities using (B)-control scheme last a longer time, which makes the adaptive weights have a better time efficiency. From Fig. 9, the actual position and heading (solid line) of the two tugs match well

Authorized licensed use limited to: TU Delft Library. Downloaded on March 04,2022 at 10:37:27 UTC from IEEE Xplore. Restrictions apply.

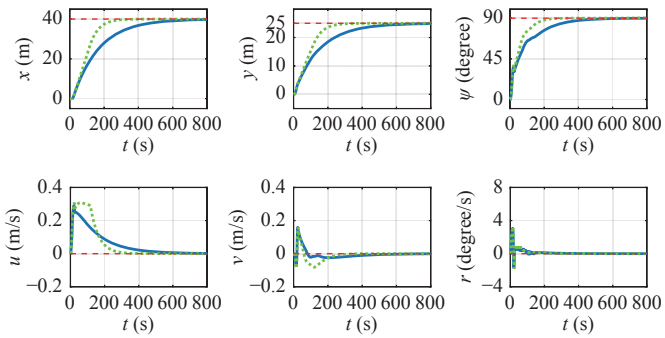

Fig. 8. Position, heading and velocities of the ship without disturbances using (A)-control scheme (solid, blue line) and (B)-control scheme (dotted, green line) algorithm; the dashed, red line represents the desired value.

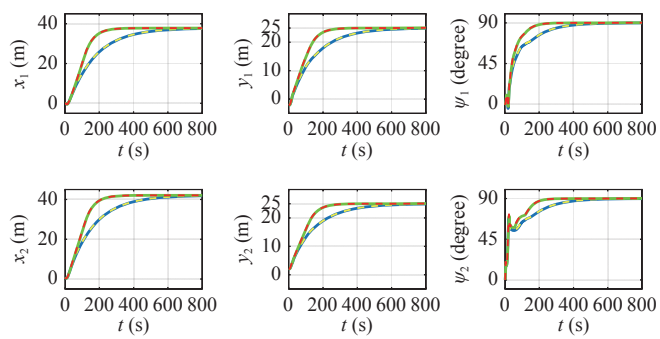

Fig. 9. Position and heading of Tug 1 (the first row) and Tug 2 (the second row) without disturbances: the solid blue line and dashed yellow line are the actual and desired values by using (A)-control scheme; the solid green line and dashed red line are the actual and desired values by using (B)-control scheme.

with their online desired values (dashed line), which reveals that the tug controllers also accomplish their tasks well.

Fig. 10 shows the control input of the ship. Fig. 10(a) illustrates the two towing angles and two towing forces, which can be seen that the four values in both schemes are within the limitation (±45° for towing angles and 3 N for towing forces). The change in towing forces using the (B)-control scheme is earlier than (A). Fig. 10(b) shows the change rate of the four control inputs, they are all within the maximum values (between the two red dashed line) as we set. Fig. 10(c) is the resultant forces and moment, whose values in both schemes converge to zero eventually.

The performance of the two algorithms can be seen in Table IV, using the following indicators: 1) Position error $e_p = |d_0 - d(t)|/d_0$; 2) Heading error $e_\psi = \left|(\psi_S(t) - \psi_{S_d})/(\psi_{S_0} - \psi_{S_d})\right|$; 3) Time cost t. The time cost is defined such that the states of the ship should satisfy all the following conditions: i) The distance from the current position to the desired position is less than half length of the ship; ii) The difference between the actual and desired heading is less than 5 degrees; iii) The surge and sway velocities are less than 0.01 m/s, the yaw velocity is less than 0.01 rad/s. It can be seen that under the similar performance of the position and heading control, the (B)-control scheme outperforms much better for the time cost.

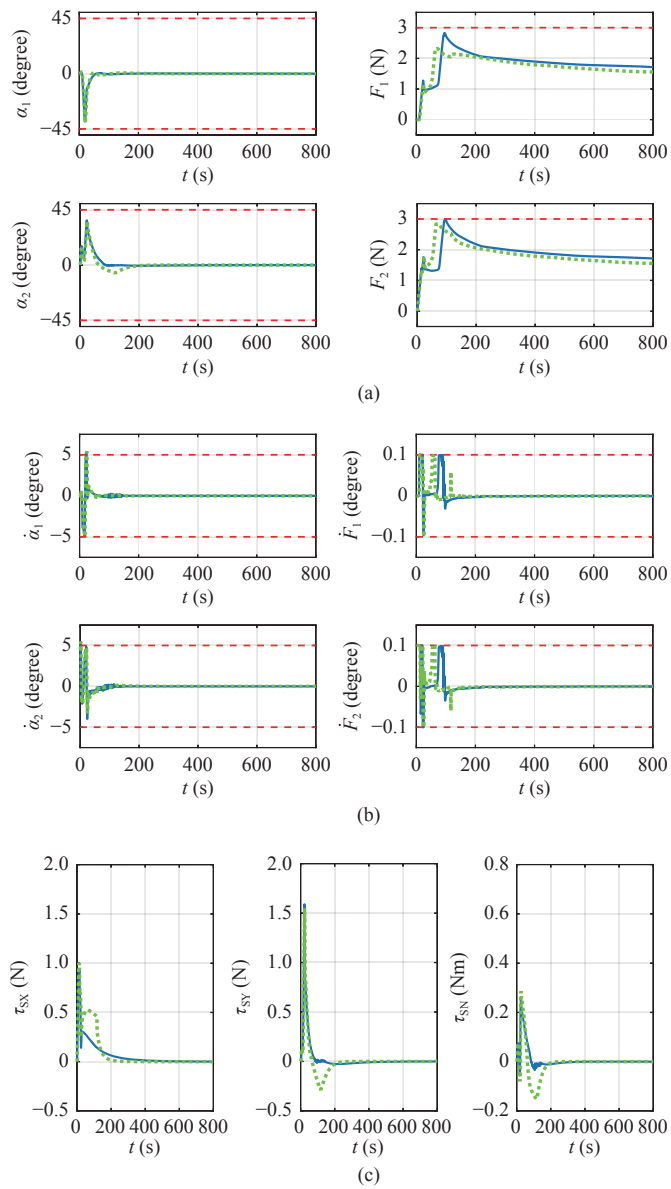

Fig. 10. Control input of the ship without disturbances using (A)-control scheme (solid, blue line) and (B)-control scheme (dotted, green line) algorithm: (a) Towing angles and forces (red dashed line is the boundary); (b) Change rate of the angles and forces (red dashed line is the boundary); (c) Resultant forces and moment.

TABLE IV
PERFORMANCE WITHOUT DISTURBANCES

Performance	Position error (e_p)	Heading error (e_ψ)	Time cost (t)
(A)-control scheme	0.53%	0.10%	712 s
(B)-control scheme	0.14%	0.20%	334 s

B. Simulation With Disturbances

The wind speed in this simulation is $V_w = 1$ m/s, the direction is $\beta_w = 45$ degrees coming from southwest. The towing process of the two algorithms are shown in Fig. 11. Compared to the (A)-control scheme, the (B)-control scheme shows better robustness. Due to the disturbances, the (A)-control scheme makes the towing system steer toward the

Authorized licensed use limited to: TU Delft Library. Downloaded on March 04,2022 at 10:37:27 UTC from IEEE Xplore. Restrictions apply.

direction of environmental effects (the combined direction of the wind and unknown effects). In this configuration, the environmental forces affecting three vessels are the minimum (the force areas above and under the waters are minimum). So the system keeps this configuration to the end. The heading of the ship is finally around 55 degrees (see the evolution of ψ in Fig. 12 blue line).

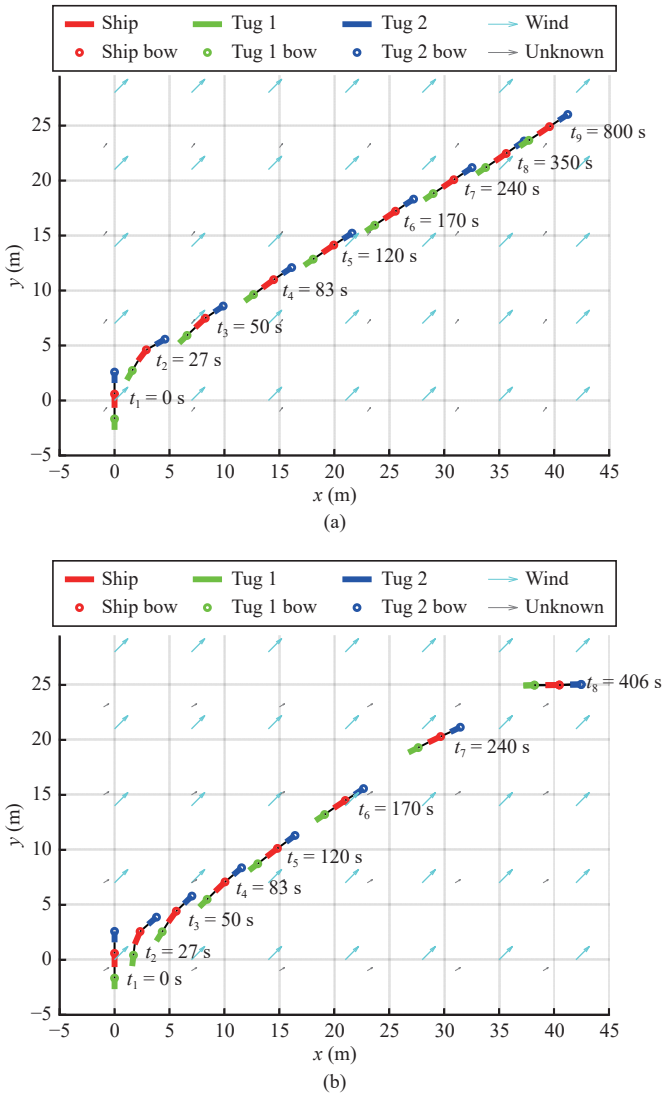

Fig. 11. Towing process of the two algorithms with disturbances: (a) (A)-control scheme; (b) (B)-control scheme.

Using the (B)-control scheme, the speed of the towing system is slower at the beginning to stabilize the ship against the wind effect. It can be observed that until $t_7 = 240$ s, the ship in Fig. 11(a) keeps ahead of that in Fig. 11(b). After that, as the adaptive weights keep reducing, the system speed is increasing. At $t_8 = 406$ s, the ship in Fig. 11(b) achieved the goal. Under the disturbances, Fig. 11(a) still shows the average position distribution, while Fig. 11(b) is characterized as dense in the beginning and sparse in the end phase. In the simulation without disturbance (Fig. 7(b)), the values of the adaptive weights are changed from $[150\ 150\ 150]^T$ to $[50\ 50\ 50]^T$, which makes the velocity control focus on the

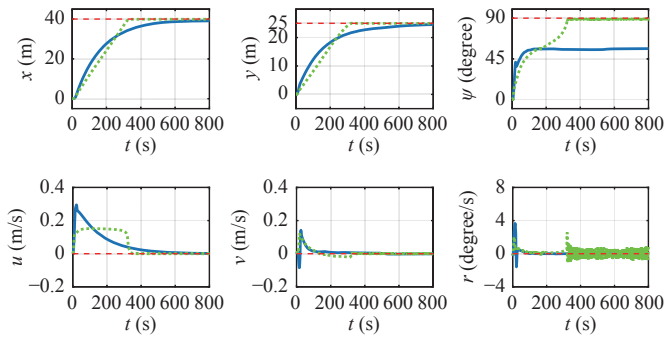

Fig. 12. Position, heading and velocities of the ship with disturbances using (A)-control scheme (solid, blue line) and (B)-control scheme (dotted, green line) algorithm; the dashed, red line represents the desired value.

beginning and end phase. In the simulation with disturbance (Fig. 11(b)), the values of the adaptive weights are changed from $[300\ 300\ 300]^T$ to $[6.5\ 6.5\ 0.5]^T$, which means that the velocity control is more concerned in the beginning phase, while the position and heading (especially the heading) control is emphasized in the end phase.

Fig. 12 shows that by using the (B)-control scheme, the position and heading of the ship can reach their desired values and the linear velocities (u and v) converge to 0. The value of angular velocity (r) has a jump at about 320 s and then starts to fluctuate. The reason for such a change is that around 320 s, the position of the ship had already reached the desired value but not for its heading. At this moment, the controller put more effort into the heading control to make the ship have a large angular velocity. After achieving the desired heading, the wind and other disturbances still exist. In this condition, however, the desired heading is not a balanced state (the balanced state should be the heading in the end phase of the (A)-control scheme, around 55 degrees). Thus, the towing system has to continuously adjust to make the ship maintain its desired heading. Fig. 13 shows that the actual position and heading of the two tugs match well with their online desired values.

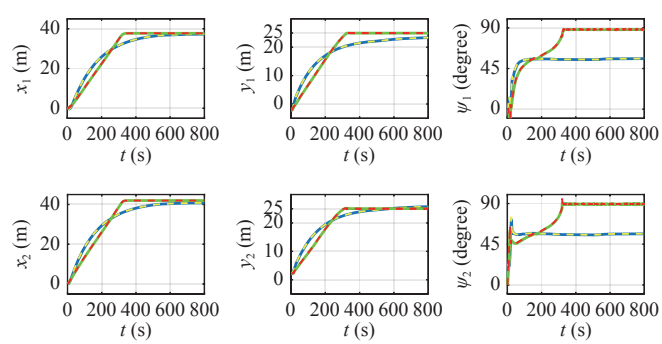

Fig. 13. Position and heading of Tug 1 (the first row) and Tug 2 (the second row) with disturbances: the solid blue line and dashed yellow line are the actual and desired values by using (A)-control scheme; the dotted green line and dashed red line are the actual and desired values by using (B)-control scheme.

The figure of control inputs (Fig. 14(a)) shows that the changes of towing angle are similar in both control scheme,

Authorized licensed use limited to: TU Delft Library. Downloaded on March 04,2022 at 10:37:27 UTC from IEEE Xplore. Restrictions apply.

the values of towing forces in the (B)-control scheme is greater than the (A)-control scheme, which reflects that the (B)-control scheme makes more effort to cope with the environmental disturbances. Despite this, the four control inputs in the (B)-control scheme are within the limitation (the green dotted line in Figs. 14(a) and 14(b) are all within the red dashed line). The value of the resultant forces and moment in Fig. 14(c), especially the and yaw moment, are not exactly zero in the end. The reason is the same as mentioned to the ship angular velocity that the ship has to compensate for the environmental effects to maintain the desired states, especially for the heading.

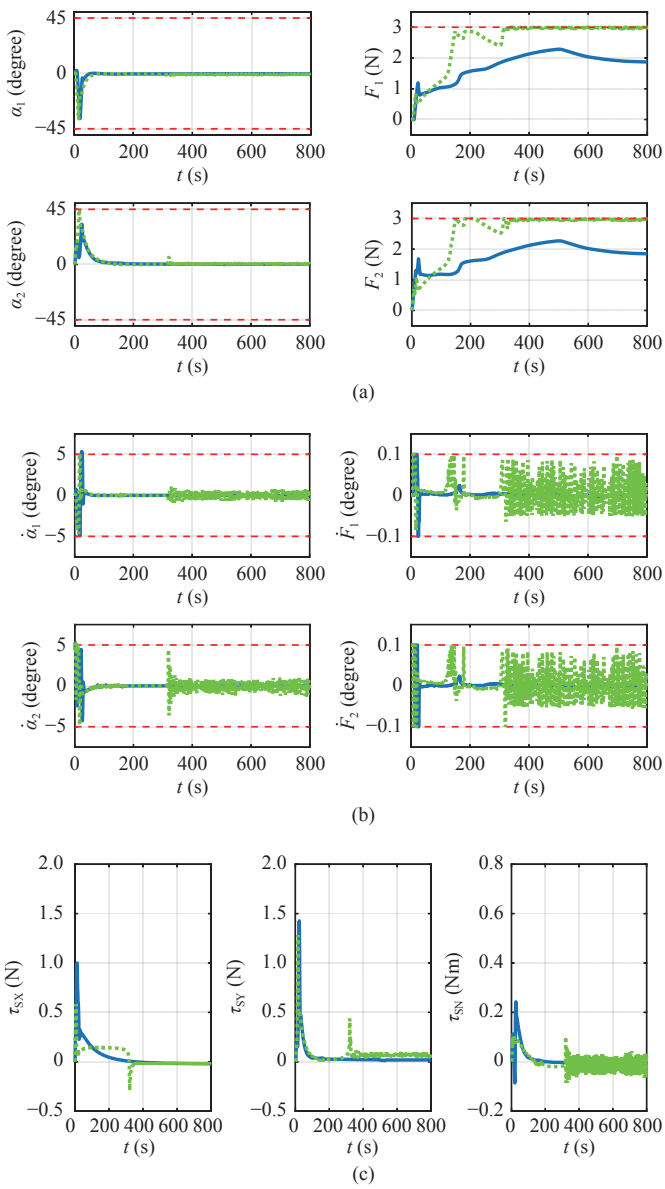

Fig. 14. Control input of the ship with disturbances using (A)-control scheme (solid, blue line) and (B)-control scheme (dotted, green line) algorithm: (a) Towing angles and forces (red dashed line is the boundary); (b) Change rate of the angles and forces (red dashed line is the boundary); (c) Resultant forces and moment.

The performance of the two control schemes in the case of simulated disturbances is shown in Table V. In this case, all the performance indexes in the (B)-control scheme outperforms than (A)-control scheme, especially for the heading control and time cost.

TABLE V
PERFORMANCE WITH DISTURBANCES

Performance	Position error (e_p)	Heading error (e_ψ)	Time cost (t)
(A)-control scheme	2.14%	37.4%	800 s**
(B)-control scheme	0.21%	0.62%	406 s

** In the whole process, the difference between the current and the desired heading of the ship is more than 5 degrees, so the time cost is the maximum computation time (800 s).

C. Simulations in Harsh Conditions

In this part, two sets of simulations are carried out to show the performance of the proposed control scheme (B) under harsh conditions.

In the first simulation, wind speed is set to be varying. As shown in Fig. 15, the first row is the wind speed varying from 1 m/s to 2 m/s. The second and third-row shows the real-time ship states, which indicates that under the condition of varying wind speed, the control scheme (B) can make sure that the ship achieves its desired position and heading. The performance indexes: position error $e_p = 0.21\%$, heading error $e_\psi = 1.65\%$, time cost $t = 472$ s.

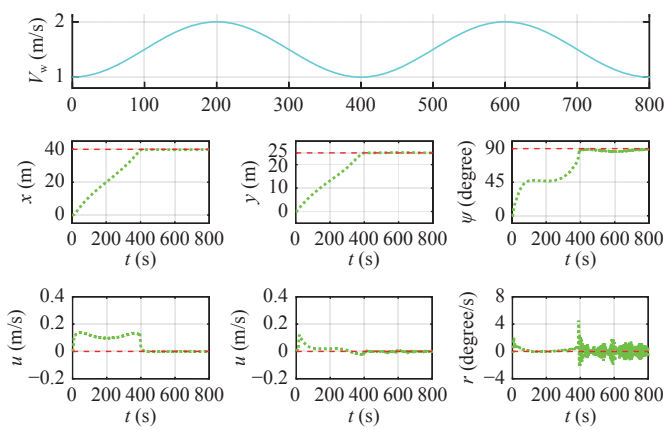

Fig. 15. Position, heading, and velocities of the ship (the second and thirdrow) under the varying wind speed (the first row) disturbances using (B)-control scheme algorithm.

In the second simulation, wind speed is set to be the maximum value (2 m/s) at all time. The performance of the (B)-control scheme with different wind directions is shown in Table VI.

When the wind direction is 0° or 180°, the position and heading control shows the best performance. Since the goal heading is vertical to the wind direction, the two tugs form the arching (0°) or sagging (180°) configuration to make the ship against the lateral forces, and this manipulation costs more time.

When the wind direction is 90° or 270°, the values of position and heading error are slightly higher, but the time

Authorized licensed use limited to: TU Delft Library. Downloaded on March 04,2022 at 10:37:27 UTC from IEEE Xplore. Restrictions apply.

TABLE VI
PERFORMANCE OF THE (B)-CONTROL SCHEME WITH SIMULATOR WIND SPEED 2 M/S

Wind direction	e_p	e_ψ	t	Final states of *** the towing system
0°	0.14%	0.26%	670 s	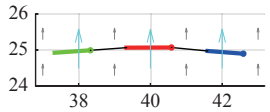
30°	0.56%	4.55%	618 s	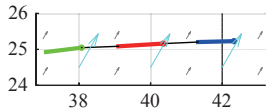
45°	0.62%	4.65%	558 s	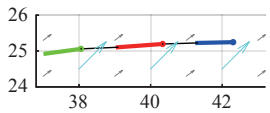
60°	0.48%	3.28%	513 s	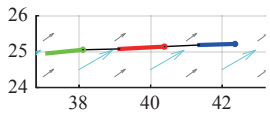
90°	0.14%	0.30%	493 s	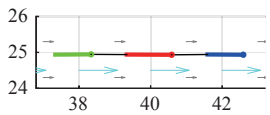
180°	0.13%	0.13%	666 s	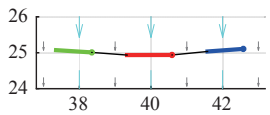
270°	0.13%	0.68%	497 s	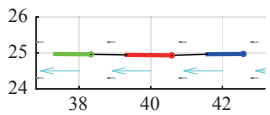

*** Blue arrows show the wind disturbances, grey arrows show the unknown disturbances.

cost is the minimum. This is because the goal heading is parallel to the wind direction, and the force area is minimum. The two tugs only have to maintain the ship velocity being zero at the goal position.

When the wind direction is 30° or 45° or 60°, it is more difficult to achieve the desired position and heading (especially the heading). The disturbance effects, on one hand, force the ship to move; on the other hand, they make the ship difficult to achieve the goal heading. So it is hard to keep the ship steady (velocity zero) and turn the ship heading to the goal direction. Despite the above difficulties, the results show that both position and heading goals are achieved within tolerance.

Based on the above simulation results, the proposed control method shows the following abilities. First, it can coordinate the two autonomous tugs to cooperatively manipulate a ship to the desired position with the desired heading. Second, it can deal with the environmental disturbances (mainly wind) even in harsh conditions. Third, it properly adjusts the ship speed according to the current ship states making the towing process time-efficient. In a real situation, once we obtain the information of the real-scaled vessel model, the proposed control method can be used to coordinate the autonomous tugs to manipulate a ship to the desired position with the desired heading under the environmental disturbances.

V. CONCLUSIONS AND FUTURE RESEARCH

This paper focuses on the cooperative control of multiple autonomous tugs for ship towing under the environmental disturbances. We propose a multi-layer multi-agent control scheme to manipulate a ship to reach a desired position with desired heading and velocity. The control scheme consists of a supervisory controller in the higher layer and two tug controllers in the lower layer.

The supervisory controller computes the desired towing forces and angles by minimizing the cost function of position and velocity errors. The weight coefficients of the position and velocity in the cost function determine the performance of control. To guarantee that the towing system functions well under environmental disturbances, an adaptive weight function is designed. By applying this weight, the controller shows disturbance robustness, time efficiency and tracking performance.

The calculated towing angles by the supervisory controller are used to compute the online reference trajectories for the autonomous tugs based on the kinematics of the ship towing system. The tug controller, on one hand, provides the towing forces to move the ship; on the other hand, it tracks the reference trajectory to reach the configuration determined by the towing angle.

Simulation experiments illustrate the performance of the proposed control scheme. When there are no disturbances, the proposed method shows more efficiency. When the motion of the towing system is affected by the wind (mainly) and unknown disturbances, the proposed method shows robustness guaranteeing that the ship is manipulated to a desired position with desired heading and velocity, even in harsh conditions.

Future research will focus on collision avoidance of the towing system. In this paper, only the meteorological environment is concerned. However, the navigation environment also has many effects on the ship manipulation. The congested waterways in port areas increases the challenges for the towing process. Thus, an efficient collision avoidance strategy is the key to ensure the safety of the ship.

REFERENCES

[1] G. Xiong, F. Zhu, X. Liu, X. Dong, W. Huang, S. Chen, and K. Zhao, "Cyber-physical-social system in intelligent transportation," *IEEE/CAA J. Autom. Sinica*, vol. 2, no. 3, pp. 320–333, 2015.

[2] R. R. Negenborn, Z. Lukszo, and H. Hellendoorn, Eds., *Intelligent Infrastructures*. Dordrecht, The Netherlands: Springer, 2010.

[3] T. M. Cioppa, T. W. Lucas, and S. M. Sanchez, "Military applications of agent-based simulations," in *Proc. Winter Simulation Conf.*, Washington DC, USA, 2004, pp. 171–180.

[4] J. E. Manley, "Unmanned surface vehicles, 15 years of development," in *Proc. OCEANS*, Quebec, Canada, 2008, pp. 1–4.

[5] M. Schiaretti, L. Chen, and R. R. Negenborn, "Survey on autonomous surface vessels: Part Ⅱ -categorization of 60 prototypes and future applications," in *Proc. Int. Conf. Computational Logistics*, Southampton, United Kingdom, 2017, pp. 234–252.

[6] X. Sun and S. S. Ge, " Adaptive neural region tracking control of multifully actuated ocean surface vessels," *IEEE/CAA J. Autom. Sinica*,

Authorized licensed use limited to: TU Delft Library. Downloaded on March 04,2022 at 10:37:27 UTC from IEEE Xplore. Restrictions apply.

vol. 1, no. 1, pp. 77–83, 2014.

[7] Y. Chen and P. Wei, " Coordinated adaptive control for coordinated path-following surface vessels with a time-invariant orbital velocity," *IEEE/CAA J. Autom. Sinica*, vol. 1, no. 4, pp. 337–346, 2014.

[8] L. Chen, H. Hopman, and R. R. Negenborn, " Distributed model predictive control for vessel train formations of cooperative multi-vessel systems," *Transportation Research Part C*: *Emerging Technologies*, vol. 92, pp. 101–118, 2018.

[9] Z. Peng, J. Wang, D. Wang, and Q.-L. Han, " An overview of recent advances in coordinated control of multiple autonomous surface vehicles," *IEEE Trans. Industrial Informatics* , vol. 17, no. 2, pp. 732–745, 2021.

[10] Y. A. Ahmed and K. Hasegawa, " Automatic ship berthing using artificial neural network based on virtual window concept in wind condition," *IFAC Proceedings Volumes* , vol. 45, no. 24, pp. 286–291, 2012.

[11] R. Zhang, P. Tang, Y. Su, X. Li, G. Yang, and C. Shi, " An adaptive obstacle avoidance algorithm for unmanned surface vehicle in complicated marine environments," *IEEE/CAA J. Autom. Sinica* , vol. 1, no. 4, pp. 385–396, 2014.

[12] A. Alop, " The main challenges and barriers to the successful "smart shipping"," *TransNav*, *the Int. Journal on Marine Navigation and Safety of Sea Transportation*, vol. 13, no. 3, pp. 521–528, 2019.

[13] H. Zheng, R. R. Negenborn, and G. Lodewijks, " Predictive path following with arrival time awareness for waterborne AGVs," *Transportation Research Part C*: *Emerging Technologies*, vol. 70, pp. 214–237, 2016.

[14] E. Zereik, M. Bibuli, N. Mišković, P. Ridao, and A. Pascoal, "Challenges and future trends in marine robotics," *Annual Reviews in Control*, vol. 46, pp. 350–368, 2018.

[15] N. Mizuno, M. Kuroda, T. Okazaki, and K. Ohtsu, "Minimum time ship maneuvering method using neural network and nonlinear model predictive compensator," *Control Engineering Practice* , vol. 15, no. 6, pp. 757–765, 2007.

[16] L. Yang and G. Chen, " Automatic berthing control of underactuated surface ships in restricted waters based on nonlinear adaptive control method," in *Proc. 31st Chinese Control Conf.*, Hefei, China, 2012, pp. 939–944.

[17] Y. A. Ahmed and K. Hasegawa, " Automatic ship berthing using artificial neural network trained by consistent teaching data using nonlinear programming method," *Engineering Applications of Artificial Intelligence*, vol. 26, no. 10, pp. 2287–2304, 2013.

[18] Y. Shuai, G. Li, X. Cheng, R. Skulstad, J. Xu, H. Liu, and H. Zhang, "An efficient neural-network based approach to automatic ship docking," *Ocean Engineering*, vol. 191, Article No. 106514, 2019.

[19] J.-Y. Park, J.-Y. Kim, NakwanPark, and N. Kim, "Design of an adaptive backstepping controller for auto-berthing a cruise ship under wind loads," *Int. Journal of Naval Architecture and Ocean Engineering*, vol. 6, no. 2, pp. 347–360, 2014.

[20] Q. Zhang, X. ku Zhang, and N. kyun Im, " Ship nonlinear-feedback course keeping algorithm based on MMG model driven by bipolar sigmoid function for berthing," *Int. Journal of Naval Architecture and Ocean Engineering*, vol. 9, no. 5, pp. 525–536, 2017.

[21] N. Mizuno, T. Kita, and T. Ishikawa, " A new solving method for nonlinear optimal control problem and its application to automatic berthing problem," in *Proc. IECON 44th Annu. Conf. IEEE Industrial Electronics Society*, Washington DC, USA, 2018, pp. 2183–2188.

[22] Z. Piao, C. Guo, and S. Sun, "Research into the automatic berthing of underactuated unmanned ships under wind loads based on experiment and numerical analysis," *Journal of Marine Science and Engineering*, vol. 7, no. 9, Article No. 300, 2019.

[23] B. Bidikli, E. Tatlicioglu, and E. Zergeroglu, " Robust dynamic positioning of surface vessels via multiple unidirectional tugboats," *Ocean Engineering*, vol. 113, pp. 237–245, 2016.

[24] M. G. Feemster and J. M. Esposito, " Comprehensive framework for tracking control and thrust allocation for a highly overactuated autonomous surface vessel," *Journal of Field Robotics* , vol. 28, no. 1, pp. 80–100, 2011.

[25] V. P. Bui, H. Kawai, Y. B. Kim, and K. S. Lee, "A ship berthing system design with four tug boats," *Journal of Mechanical Science and Technology*, vol. 25, no. 5, pp. 1257–1264, 2011.

[26] G. Sartoretti, S. Shaw, and M. A. Hsieh, " Distributed planar manipulation in fluidic environments," in *Proc. IEEE Int. Conf. Robotics and Automation*, Stockholm, Sweden, 2016, pp. 5322–5327.

[27] Y. Hu, L. Wang, J. Liang, and T. Wang, "Cooperative box-pushing with multiple autonomous robotic fish in underwater environment," *IET Control Theory & Applications*, vol. 5, no. 17, pp. 2015–2022, 2011.

[28] H. Hajieghrary, D. Kularatne, and M. A. Hsieh, "Differential geometric approach to trajectory planning: Cooperative transport by a team of autonomous marine vehicles," in *Proc. Annu. American Control Conf.*, Milwaukee, WI, USA, 2018, pp. 858–863.

[29] L. Yun and Z. Jian, "Design and implementation of cooperative turning control for the towing system of unpowered facilities," *IEEE Access*, vol. 6, pp. 18713–18722, 2018.

[30] T. D. Quan, J.-H. Suh, and Y.-B. Kim, " Leader-following control system design for a towed vessel by tugboat," *Journal of Ocean Engineering and Technology*, vol. 33, no. 5, pp. 462–469, 2019.

[31] L. Chen, H. Hopman, and R. R. Negenborn, " Distributed model predictive control for cooperative floating object transport with multi-vessel systems," *Ocean Engineering* , vol. 191, Article No. 106515, 2019.

[32] H. Yamato, " Automatic berthing by the neural controller," in *Proc. Ninth Ship Control Systems Symp.*, vol. 3, Bethesda, USA, 1990, pp. 3183–3201.

[33] A. Devaraju, L. Chen, and R. R. Negenborn, " Autonomous surface vessels in ports: Applications, technology and port infrastructures," in *Proc. 9th Int. Conf. Computational Logistics*, Vietri sul Mare, Italy, 2018, pp. 85–105.

[34] Lloyds Register, " ShipRight Procedure–Autonomous Ships," 2016. [Online]. Available: https://info.lr.org/l/12702/2016-07-07/32rrbk

[35] T. A. Johansen and T. I. Fossen, " Control allocation–A survey," *Automatica*, vol. 49, no. 5, pp. 1087–1103, 2013.

[36] J. Paulos, N. Eckenstein, T. Tosun, J. Seo, J. Davey, J. Greco, V. Kumar, and M. Yim, " Automated self-assembly of large maritime structures by a team of robotic boats," *IEEE Trans. Automation Science and Engineering*, vol. 12, no. 3, pp. 958–968, 2015.

[37] Z. Wang and V. Kumar, "Object closure and manipulation by multiple cooperating mobile robots," in *Proc. IEEE Int. Conf. Robotics and Automation*, vol. 1, Washington DC, USA, 2002, pp. 394–399.

[38] G. Eoh, J. D. Jeon, J. S. Choi, and B. H. Lee, "Multi-robot cooperative formation for overweight object transportation," in *Proc. IEEE/SICE Int. Symp. System Integration*, Kyoto, Japan, 2011, pp. 726–731.

[39] H. Hensen, *Tug Use in Port*: *A Practical Guide*. London, UK: Nautical Institute, 2003.

[40] Z. Du, V. Reppa, and R. R. Negenborn, " Cooperative control of autonomous tugs for ship towing," *IFAC-PapersOnLine* , vol. 43, no. 2, pp. 14470–14475, 2020.

[41] T. I. Fossen, *Handbook of Marine Craft Hydrodynamics and Motion Control*. Chichester, West Sussex, UK: John Wiley & Sons, 2011.

[42] K. Kepaptsoglou, G. Fountas, and M. G. Karlaftis, "Weather impact on containership routing in closed seas: A chance-constraint optimization approach," *Transportation Research Part C*: *Emerging Technologies*, vol. 55, pp. 139–155, 2015.

[43] R. R. Negenborn, " Multi-agent model predictive control with applications to power networks," Ph.D. dissertation, Delft University of Technology, 2007.

[44] A. V. Rao, " A survey of numerical methods for optimal control,"

Authorized licensed use limited to: TU Delft Library. Downloaded on March 04,2022 at 10:37:27 UTC from IEEE Xplore. Restrictions apply.

Advances in the Astronautical Sciences, vol. 135, no. 1, pp. 497–528, 2009.

[45] A. Haseltalab and R. R. Negenborn, "Model predictive maneuvering control and energy management for all-electric autonomous ships," *Applied Energy*, vol. 251, no. 113308, pp. 1–27, 2019.

[46] R. Skjetne, Ø. Smogeli, and T. I. Fossen, "Modeling, identification, and adaptive maneuvering of cybership Ⅱ: A complete design with experiments," *IFAC Proceedings Volumes*, vol. 37, no. 10, pp. 203–208, 2004.

[47] Rotterdam Port Authority, "Port information guide," Port of Rotterdam, Rotterdam, the Netherlands, techreport, May 2019. [Online]. Available: https://www.portofrotterdam.com/sites/default/files/portinformation-guide.pdf

[48] L. Moreira, T. I. Fossen, and C. G. Soares, "Path following control system for a tanker ship model," *Ocean Engineering*, vol. 34, no. 14–15, pp. 2074–2085, 2007.

[49] Z. Li and J. Sun, "Disturbance compensating model predictive control with application to ship heading control," *IEEE Trans. Control Systems Technology*, vol. 20, no. 1, pp. 257–265, 2011.

[50] F. Ding, J. Wu, and Y. Wang, "Stabilization of an underactuated surface vessel based on adaptive sliding mode and backstepping control," *Mathematical Problems in Engineering*, vol. 2013, pp. 1–5, 2013.

[51] C.-Z. Pan, X.-Z. Lai, S. X. Yang, and M. Wu, "An efficient neural network approach to tracking control of an autonomous surface vehicle with unknown dynamics," *Expert Systems with Applications*, vol. 40, no. 5, pp. 1629–1635, 2013.

[52] Y. Yang, J. Du, H. Liu, C. Guo, and A. Abraham, "A trajectory tracking robust controller of surface vessels with disturbance uncertainties," *IEEE Trans. Control Systems Technology*, vol. 22, no. 4, pp. 1511–1518, 2014.

[53] I.-A. Ihle, J. Jouffroy, and T. I. Fossen, "Robust formation control of marine craft using lagrange multipliers," in *Group Coordination and Cooperative Control*. Springer-Verlag, 2006, pp. 113–129.

[54] Y. Liu, C. Guo, and R. Zhou, "Asymptotic stabilization control of an underactuated surface vessel with optimization based on genetic algorithm," in *Proc. Second Int. Symp. Intelligent Information Technology Application*, vol. 3, Shanghai, China, 2008, pp. 622–626.

[55] L. Cavaleri, B. Fox-Kemper, and M. Hemer, "Wind waves in the coupled climate system," *Bulletin of the American Meteorological Society*, vol. 93, no. 11, pp. 1651–1661, 2012.

Zhe Du received the B.Sc. degree in maritime administration in 2015 and the M.Sc. degree in transport information engineering and control in 2018 from the Wuhan University of Technology. He is now a Ph.D. candidate at the Department of Maritime and Transport Technology, Delft University of Technology, The Netherlands. His research focuses on cooperative control of the physical-connected multi-vessel systems.

Rudy R. Negenborn received the M.Sc. degree in computer science/intelligent systems from Utrecht University in 1998, and the Ph.D. degree in distributed control for networked systems from Delft University of Technology, The Netherlands, in 2007. He is a Full Professor "Multi-Machine Operations & Logistics" at the Department of Maritime and Transport Technology, Delft University of Technology. He is also Head of the Section Trasport Engineering & Logistics in this department, and holds the scientific lead of the Researchlab Autonomous Shipping. His research interests are in the areas of distributed control, multi-controller systems, model predictive control, and optimization. He applies the developed theories to address control problems in large-scale transportation and logistic systems.

Vasso Reppa (M' 06) has been an Assistant Professor in the Department of Maritime and Transport Technology of Delft University of Technology, The Netherlands since 2018. She obtained the doctorate (2010) in electrical and computer engineering from the University of Patras, Greece. In 2009 she joined IBM Zurich Research Laboratory in Switzerland as a student intern. From 2011 to 2017, she was a Research Associate (now Research Affiliate) with the KIOS Research and Innovation Center of Excellence in Cyprus. In 2013, Dr. Reppa was awarded the Marie Curie Intra European Fellowship and worked as a Research Fellow in CentraleSupélec of the University Paris-Saclay, France from 2014 to 2016. She was a Visiting Researcher at Imperial College, the UK and at University of Newcastle, Australia in 2015 and 2016, respectively. Her current research interests include multi-level fault diagnosis and fault tolerant control, cooperative control, adaptive learning, observer-based estimation, and applications of autonomous systems in (waterborne) transport and smart buildings. Dr Reppa has been involved in several research and development projects (e.g., INTERREG "AVATAR", H2020 "NOVIMOVE", NWO "READINESS", Marie Curie ITN "AUTOBarge").

Authorized licensed use limited to: TU Delft Library. Downloaded on March 04,2022 at 10:37:27 UTC from IEEE Xplore. Restrictions apply.